



Contents lists available at ScienceDirect

Biochemical and Biophysical Research Communications

journal homepage: [www.elsevier.com/locate/ybbrc](http://www.elsevier.com/locate/ybbrc)

## Biophysical characterization reveals structural disorder in the developmental transcriptional regulator LBH

Hassan Al-Ali<sup>a</sup>, Megan E. Rieger<sup>a,b</sup>, Kenneth L. Seldeen<sup>a,b</sup>, Thomas K. Harris<sup>a</sup>, Amjad Farooq<sup>a,b</sup>, Karoline J. Briegel<sup>a,b,\*</sup>

<sup>a</sup> Department of Biochemistry & Molecular Biology, University of Miami Miller School of Medicine, Miami, FL, USA

<sup>b</sup> Braman Family Breast Cancer Institute at the Sylvester Comprehensive Cancer Center, University of Miami Miller School of Medicine, Miami, FL, USA

### ARTICLE INFO

#### Article history:

Received 1 December 2009

Available online 11 December 2009

#### Keywords:

Vertebrates

LBH

Transcriptional regulation

Embryonic development

Intrinsically disordered proteins

### ABSTRACT

Limb-bud and heart (LBH) is a key transcriptional regulator in vertebrates with pivotal roles in embryonic development and human disease. Herein, using a diverse array of biophysical techniques, we report the first structural characterization of LBH pertinent to its biological function. Our data reveal that LBH is structurally disordered with no discernable secondary or tertiary structure and exudes rod-like properties in solution. Consistent with these observations, we also demonstrate that LBH is conformationally flexible and thus may be capable of adapting distinct conformations under specific physiological contexts. We propose that LBH is a member of the intrinsically disordered protein (IDP) family, and that conformational plasticity may play a significant role in modulating LBH-dependent transcriptional processes.

© 2009 Elsevier Inc. All rights reserved.

### Introduction

Limb-bud and heart (LBH) is a highly conserved tissue-specific transcriptional regulator in vertebrates with important roles in embryonic development [1–3]. Aberrant gain-of-function of LBH, which maps to human chromosome 2p23, is associated with partial trisomy 2p syndrome, a rare human autosomal disorder with characteristic cardiovascular, skeletal and postaxial limb defects [2]. Moreover, overexpression of LBH during mouse and chick embryogenesis results in dramatic phenotypes, including cardiovascular anomalies, impaired bone formation and angiogenesis [2,3].

LBH is small nuclear acidic protein of 12.2 kDa (105 amino acids) and a theoretical isoelectric point of 4.2 that exhibits no sequence homology to any known protein families [1]. However, a conserved nuclear localization signal (NLS) and a C-terminal glutamic acid-rich putative transcriptional activation domain in the absence of a DNA-binding domain, hinted that LBH may act as a transcription cofactor [1]. This was confirmed by fusion of LBH to

**Abbreviations:** ALS, analytical laser scattering; CD, circular dichroism; GST, glutathione S-transferase; HSQC, heteronuclear single quantum coherence; IDP, intrinsically disordered protein; IPTG, isopropyl-β-D-thiogalactopyranoside; LBH, limb-bud and heart protein; NLS, nuclear localization signal; NMR, nuclear magnetic resonance; SEC, size-exclusion chromatography; SSF, steady-state fluorescence.

\* Corresponding author. Address: Department of Biochemistry & Molecular Biology, University of Miami Miller School of Medicine, 1011 NW 15th Street, Miami, FL 33136, USA. Fax: +1 305 243 9249.

E-mail address: [kbriegel@med.miami.edu](mailto:kbriegel@med.miami.edu) (K.J. Briegel).

the DNA-binding domain of GAL4, which led to transcriptional activation of a reporter gene [1,4]. Both the N-terminal and C-terminal domains of LBH are required for its transcriptional activity [4]. In heart development, LBH predominantly represses the transcriptional activities of key cardiac transcription factors Nkx2.5 and Tbx5 resulting in inhibition of the expression of a common target gene *Nppa* [2]. Furthermore, overexpression of LBH during bone development efficiently represses transcription of the key bone transcription factor Runx2 and the pro-angiogenic factor Vegf [3]. Other *in vitro* studies suggest that LBH may act synergistically with the transcriptional activators AP1 and SRF [4]. Thus, LBH appears to have both transcription co-activator and co-repressor activities. Despite the importance of LBH as a key gene regulator in human development and disease, the structural basis for the function of LBH is not understood.

In an effort to understand structure–function relationships, we overexpressed and purified full length LBH in *Escherichia coli* for biophysical characterization. Employing a diverse array of biophysical techniques, we demonstrate that native LBH is intrinsically disordered with no discernable secondary or tertiary structure exuding rod-like properties in solution. Our structural characterization of LBH provides further insight into the transcription regulator function of LBH in mechanistic terms.

### Materials and methods

**Cloning, protein expression and purification.** The murine *Lbh* open reading frame (Image Clone 6813866; ATCC) was cloned

via BamHI and SmaI sites into pGEX2T vector (Promega) using PCR technology. The pGEX2T-LBH expression vector was transformed into *E. coli* BL21 Star™ (DE3) cells (Invitrogen). A single colony of transformed cells was grown in 50 mL PG minimal medium (50 mM Na<sub>2</sub>HPO<sub>4</sub>, 50 mM KH<sub>2</sub>PO<sub>4</sub>, 5 mM Na<sub>2</sub>SO<sub>4</sub>) supplemented with 100 µg/mL carbenicillin, 2 mM MgSO<sub>4</sub>, 56 mM NH<sub>4</sub>Cl, 0.6% glucose, and 0.2× of a trace metal mixture [5] at 37 °C overnight to make a starter culture. Upon inoculation of 15 mL of starter culture in 500 mL of PG medium plus supplements, the culture was allowed to grow at 37 °C to an optical cell density of OD<sub>600</sub> = 0.8. Protein expression was induced with 0.5 mM isopropyl-β-D-thiogalactopyranoside (IPTG), and the culture was grown for an additional 4 h at 37 °C before harvesting. For <sup>15</sup>N-isotopic labeling of LBH, NH<sub>4</sub>Cl in the culture medium was replaced with an identical amount of <sup>15</sup>NH<sub>4</sub>Cl (Cambridge Isotope Laboratories Inc.). Cells (~3 g/500 mL of culture) were harvested by centrifugation, washed once in 50 mM phosphate buffer, pH 7.3, 500 mM NaCl (4 mL/g of cells), and lysed in GST-binding buffer (50 mM phosphate buffer, pH 7.3, 500 mM NaCl, 1 mM dithiothreitol; 10 mL/g of cells) using an EmulsiFlex-C3 homogenizer (Avestin Inc.). After centrifugation for 30 min at 35,000g, the soluble fraction containing the GST-LBH fusion protein was loaded at a flow rate of 1 mL/min onto tandem 5 mL GSTrap FF affinity columns (equilibrated at 4 °C in GST-binding buffer) connected to an AKTAbasic 100 Explorer FPLC system (GE Healthcare). The columns were washed with 50 mL of GST-binding buffer containing 0.01% Triton X-100, and subsequently with detergent free GST-binding buffer until the absorbance at 280 nm returned to baseline. GST-LBH protein was eluted with 50 mM Tris-HCl, pH 8.0 containing 500 mM NaCl, 2 mM dithiothreitol, and 10 mM glutathione. Fractions containing the GST-LBH protein were combined and exchanged back into GST-binding buffer using a HiPrep 26/10 desalting column (GE Healthcare). The GST affinity tag was cleaved off with 10 U of Thrombin (GE Healthcare) per mg of GST fusion protein and incubation at 4 °C for 16 h. The cleavage reaction was loaded (1 mL/min) onto the tandem GSTrap FF affinity columns, which retained cleaved GST and any uncleaved GST-LBH. The cleaved LBH that was not retained was collected, concentrated to ~1 mL using a 3K ultrafiltration concentrator (Millipore) and loaded onto a Superdex™ 75 16/60 size-exclusion column (GE Healthcare) equilibrated at 4 °C in 50 mM phosphate buffer, pH 6.5, 250 mM NaCl. LBH was separated from all other protein components by isocratic elution with this buffer at a flow rate of 1 mL/min. The purity of recombinant LBH was determined by analytical SDS-PAGE followed by Coomassie staining of the gels.

**SEC analysis.** Size-exclusion chromatography (SEC) on purified LBH was performed using a Hiload Superdex 200 column interfaced to a GE Akta FPLC system equipped with a UV detector within a chromatography refrigerator at 4 °C. The protein samples were loaded onto the column at a flow rate of 1 mL/min and the data were automatically acquired using the UNICORN software. The protein was prepared in 50 mM Tris, 200 mM NaCl, 5 mM β-mercaptoethanol and 1 mM EDTA at pH 8.0 and the starting concentrations injected onto the column were between 40–50 µM. In order to determine the observed molecular mass (*M*<sub>obs</sub>) of LBH, a calibration curve was generated by plotting the logarithm of *M*<sub>obs</sub> of a set of globular protein markers as a function of their elution volume (*V*<sub>e</sub>) and fit to linear regression according to the following relationship:

$$\text{Log}[M_{\text{obs}}] = aV_e + b \quad (1)$$

where *a* is the slope and *b* is the y-intercept of the Log[*M*<sub>obs</sub>] versus *V*<sub>e</sub> plot. The *M*<sub>obs</sub> of LBH was then calculated using Eq. (1) from the knowledge of its *V*<sub>e</sub> and the constants *a* and *b* obtained from the calibration curve.

**ALS experiments.** Analytical laser scattering (ALS) experiments were conducted on a Wyatt miniDAWN TREOS triple-angle static laser light scattering detector coupled in-line with a Wyatt Optilab rEX refractive index detector and interfaced to a Hiload Superdex 200 column under the control of a GE Akta FPLC system within a chromatography refrigerator at 4 °C. LBH samples were loaded onto the column at a flow rate of 1 mL/min and the data were automatically acquired using the ASTRA software. The protein was prepared in 50 mM Tris, 200 mM NaCl, 5 mM β-mercaptoethanol and 1 mM EDTA at pH 8.0 and the starting concentrations injected onto the column were between 40 and 50 µM. The angular- and concentration-dependence of Rayleigh scattering intensity of recombinant LBH was fit to the built-in Zimm equation [6,7]:

$$(Kc/R_\theta) = ((1/M) + 2A_2c)[1 + ((16\pi^2r^2/3\lambda^2) \sin^2(\theta/2))] \quad (2)$$

where *R*<sub>θ</sub> is the excess Rayleigh ratio due to protein in the solution as a function of protein concentration *c* (mg/mL) and the scattering angle *θ* (42°, 90° and 138°), *M* is the molecular mass of protein, *A*<sub>2</sub> is the second virial coefficient, *λ* is the wavelength of laser light in solution (658 nm), *r* is the radius of gyration of protein, and *K* is given by the following relationship:

$$K = [4\pi^2n^2(dn/dc)^2]N_A\lambda^4 \quad (3)$$

where *n* is the refractive index of the solvent, *dn/dc* is the refractive index increment of the protein in solution, *N*<sub>A</sub> is the Avogadro's number (6.022 × 10<sup>23</sup> mol<sup>-1</sup>) and *λ* is the wavelength of laser light in solution (658 nm). Weighted average values of *r* and *M* for the recombinant LBH were, respectively, calculated from the slope and the y-intercept of linear fits of a range of (*Kc/R*<sub>θ</sub>) versus sin<sup>2</sup>(*θ*/2) plots for a total of 480 data slices in the limit of low protein concentrations along the elution profile at three scattering angles as described previously [6,7].

**CD studies.** Circular dichroism (CD) measurements were conducted on a Bio-Logic MOS450 spectrometer equipped with a CD accessory and thermostatically controlled with a water bath. All data were acquired on a 10 µM LBH in 50 mM sodium phosphate at pH 8.0 and processed using the Biokine software. CD spectra were collected at 25 °C using a quartz cuvette with a 2-mm pathlength in the wavelength range 180–300 nm and normalized against a reference spectrum to remove the buffer contribution. The reference spectrum of the buffer was obtained in a similar manner. Data were recorded with a slit bandwidth of 2 nm at a scan rate of 3 nm/min. The data set represents an average of four scans acquired at 1 nm intervals.

**SSF measurements.** Steady-state fluorescence (SSF) spectra were collected on a Jasco FP-6500 spectrofluorometer using a 5-mm pathlength cuvette at 25 °C. Emission spectra were acquired from 300 to 500 nm using an excitation wavelength of 295 nm and a 3-nm bandwidth for both excitation and emission. Data were collected on a 10 µM LBH in 50 mM phosphate, 0.1 mM β-mercaptoethanol containing either 50 or 250 mM NaCl at pH 6.5. Fluorescence spectra of the buffer solution were recorded and subtracted from the protein spectra.

**NMR spectroscopy.** For nuclear magnetic resonance (NMR) analysis, 0.5 mM <sup>15</sup>N-isotopic labeled LBH was prepared in 50 mM phosphate, pH 6.5, 250 mM NaCl, and 5% D<sub>2</sub>O. Two-dimensional <sup>1</sup>H-<sup>15</sup>N HSQC spectra were collected at 25 °C with a Bruker DMX500 NMR spectrometer (500 MHz for protons) equipped with pulsed-field gradients, four frequency channels, and a triple resonance cryoprobe with an actively shielded z-gradient. For the <sup>1</sup>H-<sup>15</sup>N HSQC experiment, the data were recorded by using a pulse sequence in which the HSQC detection scheme was optimized to avoid water saturation [8] and by using the States-TPP1 method [9] in the indirect dimension, with a relaxation delay of 1 s. The data were obtained with spectral widths of 1520 and 7000 Hz in *f*<sub>1</sub> (<sup>15</sup>N) and *f*<sub>2</sub> (<sup>1</sup>H), respectively, and with 256 and 1024 complex

points, respectively, in the  $t_1$  and  $t_2$  dimensions. A total of eight transients were acquired for each hypercomplex  $t_1$  point with  $^1\text{H}$  and  $^{15}\text{N}$  carriers positioned at 4.71 and 120 ppm, respectively. The program NMRPipe [10] was used to process the data. Proton chemical shifts are given with respect to the HDO signal taken to be 4.71 ppm relative to external TSP (0.0 ppm) at 25 °C. The  $^{15}\text{N}$  chemical shifts were indirectly referenced.

**Structural order and disorder prediction.** The relative order/disorder of the amino acid composition of LBH was predicted by the neural network program PONDR® VL-XT [11,12], which is available from Molecular Kinetics Inc. at <http://www.pondr.com>.

## Results and discussion

### Recombinant LBH can be purified to apparent homogeneity

In order to facilitate biophysical studies aimed at elucidating the mechanisms by which LBH modulates transcriptional processes, we overexpressed and purified mammalian LBH protein from *E. coli*. The protocol we developed (see Materials and methods) reproducibly yielded 20–30 mg of purified full length LBH from 1 L of culture, which was of  $\geq 95\%$  homogeneity as judged by SDS–PAGE (Fig. 1B, lane 5). It should be noted that the recombinant LBH additionally contains N-terminal Gly-Ser residues as a

result of using a pGEX2T expression vector (Fig. 1A) and has a theoretical molecular mass of 12.3 kDa.

### Hydrodynamic analysis reveals that LBH lacks a globular fold

In an effort to gain an insight into the globular fold of LBH, we conducted a detailed size-exclusion chromatography (SEC) analysis (Fig. 2A). Interestingly, our data reveal that LBH elutes with an apparent molecular mass of about 33 kDa using a set of globular proteins as reference. This value is approximately threefold greater than its theoretical molecular mass of 12.3 kDa and could suggest that LBH exists as a higher-order oligomer in solution. However, since determination of molecular mass of proteins from such analysis is highly dependent upon their globular shape, an alternative scenario could be that LBH lacks an intrinsic globular fold allowing it to behave as a structurally disordered polymer. To distinguish between these two possibilities, we carried out analytical laser scattering (ALS) measurements (Fig. 2B). Fit of these data to Zimm equation yielded values of  $11.8 \pm 0.5$  kDa and  $234 \pm 6$  Å for the molecular mass and radius of gyration for the recombinant LBH, respectively. Thus, the molecular mass determined for LBH from ALS analysis on the basis of first principles of hydrodynamics is in an excellent agreement with a theoretical value of 12.3 kDa and suggests that LBH exists as a monomer in solution. Additionally, a value of 234 Å for the radius of gyration of LBH strongly suggests that LBH lacks a globular fold and most likely behaves as a rod-like macromolecule. Given that structural disorder is a hallmark of eukaryotic transcriptional regulators [13,14], the possibility that LBH may belong to what have come to be known as intrinsically disordered proteins (IDPs) [15] deserved further investigation.

### Spectroscopic studies indicate that LBH lacks secondary and tertiary structural features

To further investigate the extent to which LBH may be structurally disordered, we carried out steady-state fluorescence (SSF) and circular dichroism (CD) measurements (Fig. 3A and B). Consistent with the above observations, SSF and CD data further indicate that recombinant LBH is largely unfolded. In Fig. 3A, fluorescence spectrum of LBH shows that the single tryptophan residue (Trp-80) within the protein emits with  $\lambda_{\text{max}}$  around 350 nm. Given that this is the  $\lambda_{\text{max}}$  observed for free tryptophan residues in solution, it can be argued that the tryptophan residue within LBH is completely accessible to the aqueous solvent and that LBH is likely to contain a non-globular fold. That this is the case is further corroborated by CD measurements. As shown in Fig. 3B, CD spectrum of LBH in the far-UV region (180–240 nm) is largely characterized by a negative band centered around 200 nm, which is reminiscent of a structurally disordered protein with little or no secondary structure. Additionally, the CD spectrum of LBH in the near-UV region (240–300 nm) is completely devoid of a band around 280 nm, which would be expected for a non-globular protein with one or more tryptophan residues. Taken together, our SSF and CD data argue strongly that LBH lacks any discernable secondary or tertiary structure.

### NMR analysis shows that LBH may exist in multiple conformations

In order to further assess the relative degree of structural disorder in LBH, we also measured its two-dimensional  $^1\text{H}$ – $^{15}\text{N}$  HSQC NMR spectrum (Fig. 3C). In this analysis, the  $^1\text{H}$  and  $^{15}\text{N}$  chemical shifts ( $\delta$ ) of directly bonded  $^1\text{H}$ – $^{15}\text{N}$  pairs (i.e., backbone and side chain amide groups) are correlated. As shown in Fig. 3C, the majority of backbone amide proton resonances exhibited poor chemical shift dispersion ( $\sim 7.9$ – $8.7$  ppm), indicating substantial regions of structural disorder. In addition, many resonances were broadened,

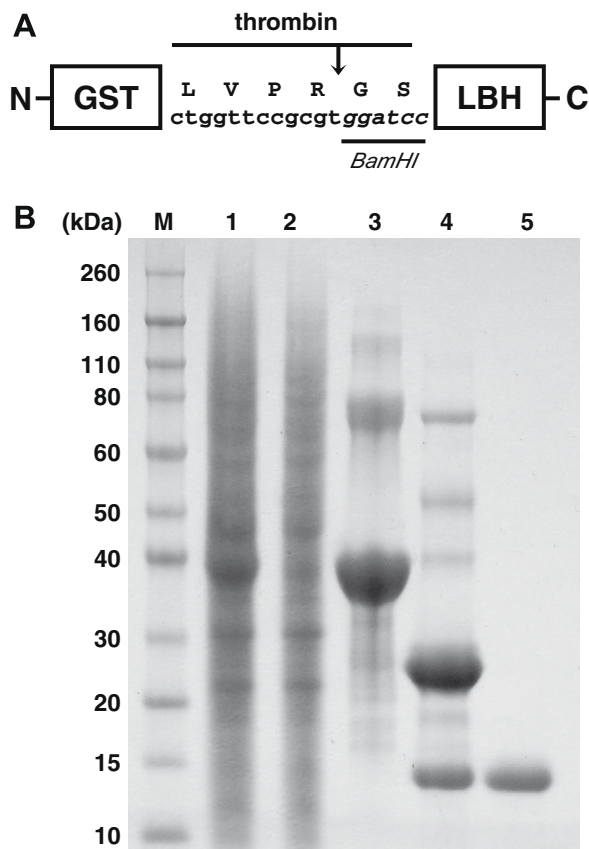


**Fig. 1.** Purification of recombinant LBH from *E. coli*. (A) Coding region of the recombinant pGEX2T-LBH expression vector depicting the thrombin cleavage site and the BamHI restriction enzyme recognition sequences (italics) used to directionally clone the LBH coding region into pGEX2T. (B) SDS–PAGE analysis with Coomassie staining. M, molecular weight standard; lane 1, total soluble lysate; lane 2, proteins from the soluble lysate that were not retained on the GST Sepharose High Trap HP affinity column; lane 3, proteins that were retained and subsequently eluted from the GSTrap HP affinity column; lane 4, protein products after thrombin digestion; lane 5, purified LBH resolved by Superdex™ 75 size-exclusion chromatography.

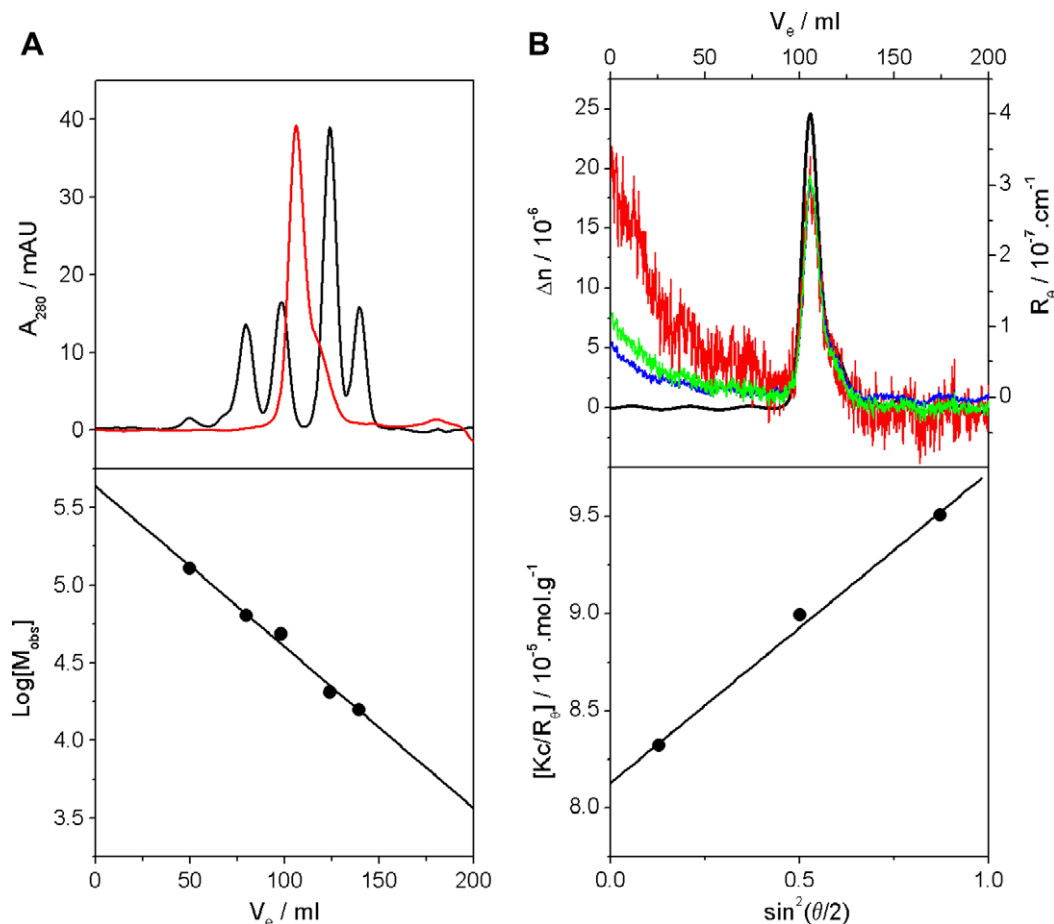


**Fig. 2.** Hydrodynamic studies of LBH. (A) SEC analysis of LBH. In the upper panel, elution profile of LBH (red) is superimposed upon the elution profiles of globular protein markers (black). Note that the elution of LBH and protein markers were recorded at 280 nm ( $A_{280}$ ) using a UV monitor. In the lower panel, a plot of the logarithm of the observed molecular mass ( $M_{\text{obs}}$ ) of known protein markers versus their elution volume ( $V_e$ ) is shown. The data points in the order of increasing  $V_e$  and decreasing  $\text{Log}[M_{\text{obs}}]$  correspond to 128-kDa dimeric albumin, 64-kDa monomeric albumin, 48-kDa ovalbumin, 20-kDa chymotrypsinogen; 16-kDa ribonuclease, respectively. The solid line through the data points represents a linear fit to Eq. (1). (B) ALS analysis of LBH. In the upper panel, the differential refractive index ( $\Delta n$ ) of LBH (black) is superimposed upon the extent of its scattering intensity, expressed in terms of the excess Rayleigh ratio ( $R_\theta$ ), at three scattering angles of  $42^\circ$  (red),  $90^\circ$  (green) and  $138^\circ$  (blue) as a function of elution volume ( $V_e$ ). Note that  $\Delta n$  is a dimensionless parameter expressed here in absolute terms. In the lower panel, a representative plot of  $[Kc/R_\theta]$  versus  $\sin^2(\theta/2)$  is shown at a protein concentration corresponding to the maximum values of  $R_\theta$  at the three scattering angles. The solid line through the data points represents a linear fit to Eq. (2). (For interpretation of the references to color in this figure legend, the reader is referred to the web version of this paper.)

indicating interconversion between multiple conformations occurring within the “intermediate” NMR timescale. Since the amide nitrogen present in the side chains of both Gln and Asn contains two bonded protons ( $-\text{NH}_2$ ), this group yields a pair of resonances with the same  $^{15}\text{N}$  chemical shift but different  $^1\text{H}$  chemical shifts. Thus, pairs of resonances are observed in the upfield regions (Fig. 3C,  $^{15}\text{N}\delta \sim 113$  ppm and  $^1\text{H}\delta \sim 6.9$  ppm and  $\sim 7.7$  ppm), as expected for the  $-\text{NH}_2$  group in the side chains of the 3 Asn and 4 Gln residues (Fig. 4A, N24, N94, N100, Q43, Q88, Q92, and Q105). Interestingly, a pair of resonances was observed in the downfield regions (Fig. 3C,  $^{15}\text{N}\delta = 129$  ppm and  $^1\text{H}\delta = 10.1$  ppm) for the NεH of the aromatic indole side chain of the single tryptophan (Trp-80), indicating slow exchange between two different conformations. Taken together, our NMR analysis suggests that LBH may not only be structurally disordered but that it may also exhibit conformational flexibility allowing it to exist in multiple conformations.

*In silico* analysis confirms that LBH is largely disordered with little propensity for globular fold

There is growing evidence that IDPs exhibit notable structural features at the primary sequence level [11,12,15,16]. Indeed, bioinformatics analysis of the primary amino acid composition of LBH re-

vealed an enrichment of disorder-promoting residues (Fig. 4A). These include nearly 35% of charged residues (Arg/Lys/Glu/Asp), 10% of polar residues (Ser/Thr) and another 15% of helix breakers (Pro/Gly). On the other side, LBH is severely devoid of hydrophobic residues (Met/Leu/Ile/Val) that dominate in globular proteins. It should be noted that such tendency of LBH for intrinsic disorder is highly conserved among all vertebrate LBH orthologues (Fig. 4A). The LBH amino acid sequence was further subjected to computer analysis using the PONDR<sup>®</sup> VL-XT software, which utilizes a set of neural network predictors to calculate the probability that amino acid residues exist in either structurally ordered or disordered peptide regions (Fig. 4B) [11,12]. As displayed in Fig. 4B, 70 of 105 LBH residues (approximately 67%) are predicted to be disordered and are located primarily in two peptide regions spanning residues 15–38 and 60–105. Interestingly, the predicted NLS (residues 56–63) of LBH overlaps with the most ordered region spanning residues 39–59, whereas the Glu-rich putative transcriptional activation domain (residues 67–104) resides in the longest disordered region.

## Conclusion

We have purified and biophysically characterized the mammalian LBH protein expressed in *E. coli*, which is a representative of



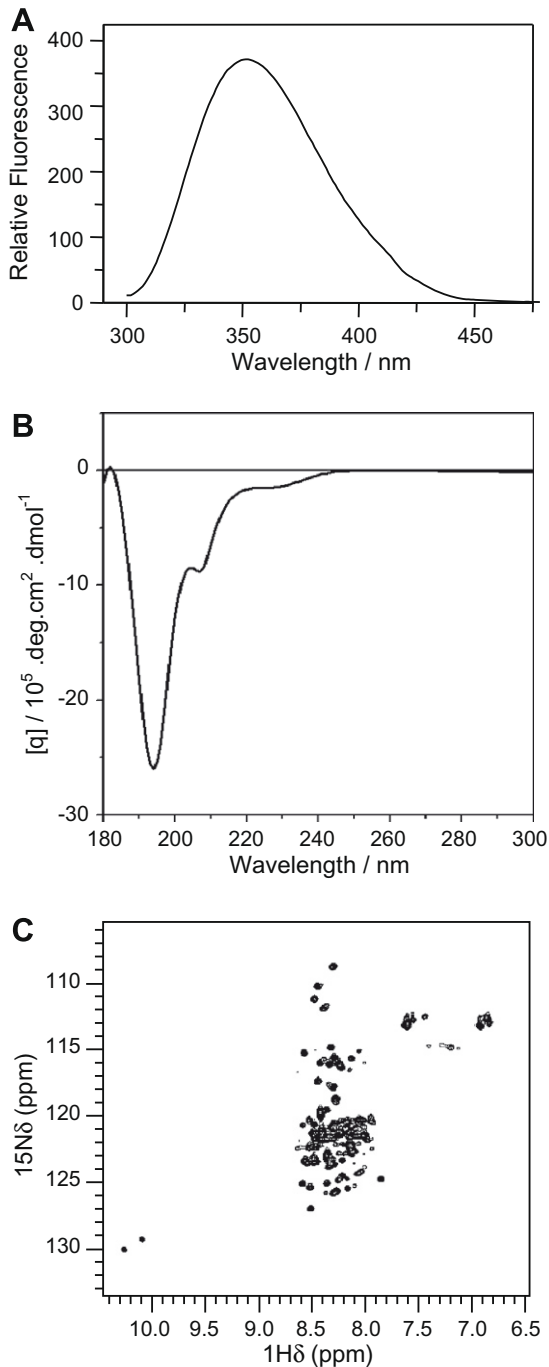


**Fig. 3.** Spectroscopic characterization of LBH. (A) Tryptophan fluorescence spectrum of LBH. (B) CD spectrum of LBH.  $[\theta]$  represents the molar ellipticity defined by the equation:  $[\theta] = (10^5 \Delta A / cl)$ , where  $\Delta A$  is the difference between the absorbance of left circularly polarized and right circularly polarized light in mdeg (the observed ellipticity),  $c$  is the protein concentration in  $\mu\text{M}$  and  $l$  is the cuvette pathlength in cm. (C) Two-dimensional  $^1\text{H}$ - $^{15}\text{N}$  HSQC NMR spectrum of uniform  $^{15}\text{N}$ -isotopic labeled LBH. The final concentration of LBH was 0.5 mM in 50 mM phosphate buffer, pH 6.5, containing 250 mM NaCl and 5%  $\text{D}_2\text{O}$ . Spectra were collected at 25 °C with a Bruker DMX500 NMR spectrometer (500 MHz for protons) equipped with a triple resonance cryoprobe.

the vertebrate LBH transcription cofactor family. Our data reveal that native LBH is a monomeric protein with a high degree of structural intrinsic disorder that exhibits multiple traits of IDPs. IDPs fulfill key molecular recognition functions in transcriptional regulation, DNA repair and cell signaling [13–15,17], and are abundantly represented among proteins associated with human disease [18,19]. This is noteworthy as abnormal LBH gain-of-func-

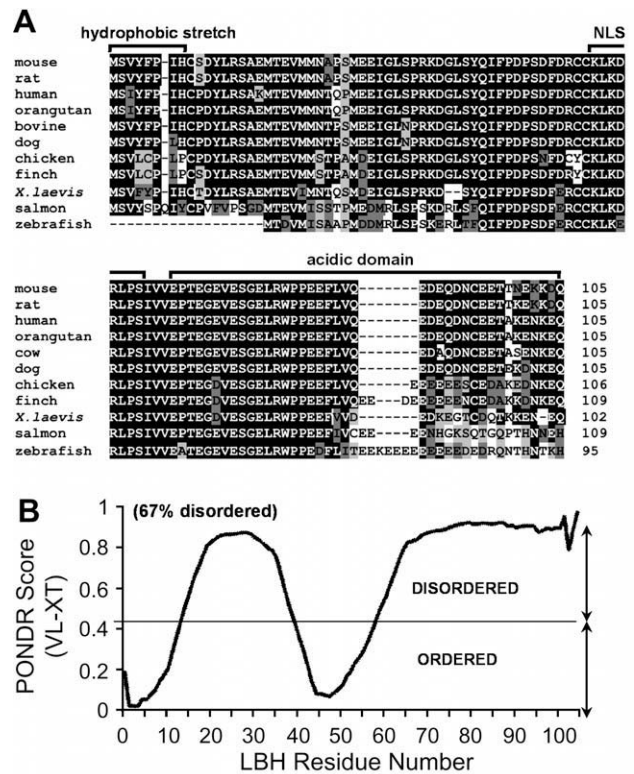


**Fig. 4.** In silico analysis of LBH. (A) Sequence alignment of LBH proteins from mouse (NCBI ID: NP\_084275.3), rat (NP\_001123352.1), human (NP\_112177.2), orangutan (NP\_001125165.1), bovine (NP\_001092622.1), dog (XP\_853968.1), chicken (NP\_001026209.1), finch (XP\_002198437.1), *Xenopus laevis* (NP\_001081507.1), salmon (ACI34372.1) and zebrafish (NP\_956814.1) showing a high degree of conservation (58–99%) of disorder-promoting amino acid residues in LBH proteins across vertebrate species. Dark shading represents identity at a given amino acid residue, whereas light shading represents amino acid residue similarity. Conserved protein motifs predicted by the primary amino acid sequence [1] are shown on the top of the alignment. NLS, nuclear localization signal. (B) PONDR® VL-Xt analysis. Amino acids with PONDR scores  $\geq 0.5$  are classified as being in 'disordered' peptide regions and those with scores  $< 0.5$  are classified as being in 'ordered' peptide regions.

tion is implicated in human congenital heart disease [2]. Taken together, our data suggest that conformational plasticity may play a significant role in LBH transcriptional regulator function, as it allows LBH to form multi-partner interactions with different transcription factor classes. Finally, like other IDPs, LBH may undergo a 'disorder-to-order' transition upon binding to its target molecules, and, depending on the target-induced conformational changes, may acquire different functional activities.

#### Acknowledgments

This work was supported by the James and Esther King Biomedical Program of the Florida State Department of Health (NIR05-01-5186 to K.J.B.), the Braman Family Breast Cancer Institute of the UM Sylvester Comprehensive Cancer Center (K.J.B. and A.F.), the National Institute of Health (RO1-GM69868 to T.K.H.; RO1-GM083897 to A.F.), and a Department of Defense pre-doctoral fellowship (W81XWH-08-1-0253 to M.E.R.).

#### References

- [1] K.J. Briegel, A.L. Joyner, Identification and characterization of Lbh, a novel conserved nuclear protein expressed during early limb and heart development, *Dev. Biol.* 233 (2001) 291–304.
- [2] K.J. Briegel, H.S. Baldwin, J.A. Epstein, A.L. Joyner, Congenital heart disease reminiscent of partial trisomy 2p syndrome in mice transgenic for the transcription factor Lbh, *Development* 132 (2005) 3305–3316.

- [3] K.L. Conen, S. Nishimori, S. Provot, H.M. Kronenberg, The transcriptional cofactor Lbh regulates angiogenesis and endochondral bone formation during fetal bone development, *Dev. Biol.* 333 (2009) 348–358.
- [4] J. Ai, Y. Wang, K. Tan, Y. Deng, N. Luo, W. Yuan, Z. Wang, Y. Li, X. Mo, C. Zhu, Z. Yin, M. Liu, X. Wu, A human homolog of mouse Lbh gene, hLBH, expresses in heart and activates SRE and AP-1 mediated MAPK signaling pathway, *Mol. Biol. Rep.* 35 (2007) 179–187.
- [5] F.W. Studier, Protein production by auto-induction in high density shaking cultures, *Protein Expr. Purif.* 41 (2005) 207–234.
- [6] B. Zimm, The scattering of light and the radial distribution function of high polymer solutions, *J. Chem. Phys.* 16 (1948) 1093–1099.
- [7] P. Wyatt, Light scattering and the absolute characterization of macromolecules, *Anal. Chim. Acta* 272 (1993) 1–40.
- [8] S. Mori, C. Abeygunawardana, M.O. Johnson, P.C. van Zijl, Improved sensitivity of HSQC spectra of exchanging protons at short interscan delays using a new fast HSQC (FHSQC) detection scheme that avoids water saturation, *J. Magn. Reson. B* 108 (1995) 94–98.
- [9] D. Marion, P.C. Driscoll, L.E. Kay, P.T. Wingfield, A. Bax, A.M. Gronenborn, G.M. Clore, Overcoming the overlap problem in the assignment of  $^1\text{H}$  NMR spectra of larger proteins by use of three-dimensional heteronuclear  $^1\text{H}$ - $^{15}\text{N}$  Hartmann–Hahn-multiple quantum coherence and nuclear Overhauser-multiple quantum coherence spectroscopy: application to interleukin 1 beta, *Biochemistry* 28 (1989) 6150–6156.
- [10] F. Delaglio, S. Grzesiek, G.W. Vuister, G. Zhu, J. Pfeifer, A. Bax, NMRPipe: a multidimensional spectral processing system based on UNIX pipes, *J. Biomol. NMR* 6 (1995) 277–293.
- [11] X. Li, P. Romero, M. Rani, A.K. Dunker, Z. Obradovic, Predicting protein disorder for N-, C-, and internal regions, *Genome Inf. Ser. Workshop Genome Inform.* 10 (1999) 30–40.
- [12] P. Romero, Z. Obradovic, X. Li, E.C. Garner, C.J. Brown, A.K. Dunker, Sequence complexity of disordered protein, *Proteins* 42 (2001) 38–48.
- [13] A.L. Fink, Natively unfolded proteins, *Curr. Opin. Struct. Biol.* 15 (2005) 35–41.
- [14] M. Fuxreiter, P. Tompa, I. Simon, V.N. Uversky, J.C. Hansen, F.J. Asturias, Malleable machines take shape in eukaryotic transcriptional regulation, *Nat. Chem. Biol.* 4 (2008) 728–737.
- [15] A.K. Dunker, M.S. Cortese, P. Romero, L.M. Iakoucheva, V.N. Uversky, Flexible nets. The roles of intrinsic disorder in protein interaction networks, *FEBS J.* 272 (2005) 5129–5148.
- [16] V.N. Uversky, C.J. Oldfield, A.K. Dunker, Showing your ID: intrinsic disorder as an ID for recognition, regulation and cell signaling, *J. Mol. Recognit.* 18 (2005) 343–384.
- [17] V. Vacic, C.J. Oldfield, A. Mohan, P. Radivojac, M.S. Cortese, V.N. Uversky, A.K. Dunker, Characterization of molecular recognition features, MoRFs, and their binding partners, *J. Proteome Res.* 6 (2007) 2351–2366.
- [18] L.M. Iakoucheva, C.J. Brown, J.D. Lawson, Z. Obradovic, A.K. Dunker, Intrinsic disorder in cell-signaling and cancer-associated proteins, *J. Mol. Biol.* 323 (2002) 573–584.
- [19] V.N. Uversky, C.J. Oldfield, U. Midic, H. Xie, B. Xue, S. Vucetic, L.M. Iakoucheva, Z. Obradovic, A.K. Dunker, Unfoldomics of human diseases: linking protein intrinsic disorder with diseases, *BMC Genomics* 10 (Suppl. 1) (2009) S7.